

# Transport properties of a disordered chain of Majorana fermions

von

Christoph Thomas Baumann

Bachelorarbeit in Physik

vorgelegt der

Fakultät für Mathematik, Informatik und Naturwissenschaften  
der RWTH Aachen

im September 2012

angefertigt im

Institut für Quanteninformation

bei

Herrn Prof. Dr. Fabian Hassler

# Contents

<b>1</b>	<b>Introduction</b>	<b>3</b>
<b>2</b>	<b>Majorana fermions</b>	<b>4</b>
2.1	What are Majorana fermions? . . . . .	4
2.2	Majorana fermions in Kitaev's toy model . . . . .	6
2.3	Bogoliubov Transformation . . . . .	8
<b>3</b>	<b>Majorana fermions with disorder</b>	<b>16</b>
3.1	Low-energy Kitaev model . . . . .	16
3.2	Scattering matrix . . . . .	18
3.3	Relation between the reflection matrix and the topological quantum number . . . . .	22
3.4	Disorder . . . . .	24
3.5	Result . . . . .	24
<b>4</b>	<b>Conclusion and Outlook</b>	<b>29</b>
	<b>Bibliography</b>	<b>30</b>
<b>A</b>	<b>Appendix</b>	<b>31</b>
A.1	Scattering theory . . . . .	31
A.2	Determinantal condition for orthogonal matrices . . . . .	32

# 1 Introduction

The thesis deals with the topic of Majorana fermions. Majorana fermions constitute an interesting field of modern condensed matter physics, since they coincide with their own antiparticle and they appear as *zero-energy* modes, e.g., in superconducting systems. The existence of *zero-energy* modes causes that the superconducting systems can be realized in two different phases, differed by the absence or presence of unpaired Majorana fermions at the end of the system. The main interested is focused on the appearance of unpaired Majorana modes. The possibility of obeying non-Abelian statistics allows applications to topological quantum computation and is part of present research.

In particular, we will discuss the existence of unpaired Majorana fermions in the low-energy version of Kitaev's toy model in presence of disorder, but we will start with an introduction of Majorana fermions, where we will define the main properties and we will show that Majorana zero modes can be presented as a superposition of conventional fermions. Subsequently, we will introduce Kitaev's toy model [1] and we will study the system with open and periodic boundary conditions to show the appearance of Majorana fermions.

In addition, we will relate the topological quantum number to the determinant of the reflection matrix, which enables us the possibility to study the disordered system with the methods of scattering theory. In the main part, we will discuss the low-energy version of Kitaev's model in presence of disorder, and we will determine a phase diagram, which illustrates the appearance of unpaired Majorana fermions with respect to the strength of disorder.

## 2 Majorana fermions

In this chapter, we will introduce Majorana fermions and we will mention their main characteristics. Afterwards, we will introduce Kitaev's toy model and we will study the system with respect to Majorana fermions. We will study the model with open and periodic boundary conditions and we will argue under what conditions, we have the ability to observe unpaired Majorana fermions in this simple model.

### 2.1 What are Majorana fermions?

In 1937, Ettore Majorana studied the Dirac equation, whose solutions are in general complex-valued. The complex-valued solutions describe relativistic particles with spin- $\frac{1}{2}$  that are called Dirac-fermions. During his study, Majorana made a basis change of Dirac's equation and found real solutions with a new property that represent Majorana fermions [2]. These Majorana fermions are characterized through the fact that they coincide with their own antiparticle.

Unlike to high-energy physics, where Majorana fermions are fundamental particles, we are able to generate spinless *zero-energy* modes in solid state systems and in the following, we equalize the meaning of Majorana fermion and a *zero-energy* mode. In condensed matter physics, the following relation for the operator generating the particles reads

$$\gamma_{\alpha,x} = \gamma_{\alpha,x}^\dagger, \quad \{\gamma_{\alpha,x}, \gamma_{\alpha',x'}\} = 2\delta_{\alpha,\alpha'}\delta_{x,x'}. \quad (2.1)$$

The relation on the right-hand side describes the usual anticommutation rule, Majorana fermions obey. The relation on the left-hand side symbolizes the fact that Majorana fermions coincide with their own antiparticles, which describes the main characteristic of a Majorana fermion. To understand the equality of Majorana fermions and *zero-energy* modes, we need to derive a link between creation and annihilation operators. Therefore, we argue that Majorana fermions only emerge in systems that have particle-hole symmetry in the associated Bogoliubov-de Gennes Hamiltonian. The particle-hole symmetry indicates that we treat the system with respect to particle and hole excitations (the hole excitation plays the role of an antiparticle), since the

annihilation of a particle corresponds to the creation of an antiparticle. In Sec. 2.3, we will see that particle excitations belong to an energy  $E$ , while hole excitations belong to an energy  $-E$ . Thus, we conclude that the creation and annihilation operators are related through

$$\gamma(E) = \gamma^\dagger(-E), \quad (2.2)$$

where  $\gamma(E)$  annihilates a particle of energy  $E$  and  $\gamma^\dagger(-E)$  creates an antiparticle [3]. For an energy  $E = 0$ , particle and antiparticle coincide and we obtain Majorana fermions. Since particle and antiparticle only coincide at  $E = 0$ , Majorana fermions only exist as *zero-energy* modes and we have determined the equality in solid state systems.

After defining the main typical properties of Majorana fermions, we show that Majorana fermions are not only a theoretical definition. In fact, conventional fermions can be built up of a superposition of Majorana fermions and vice versa. The following relation shows the superimposed Majorana operators [4]:

$$c_x = \frac{1}{2}(\gamma_{B,x} + i\gamma_{A,x}), \quad (2.3)$$

where  $c_x$  describes the annihilation operator of a spinless fermion at position  $x$  and  $\gamma_{A,x}$ ,  $\gamma_{B,x}$  describe the Majorana operators at position  $x$ . Looking at Eq. (2.3), it is not evident that the operators  $\gamma_{A,x}$ ,  $\gamma_{B,x}$  coincide with their Hermitian conjugate and that they obey the usual anticommutation rule for Majorana fermions. To ensure that the  $\gamma$ -operators represent Majoranas, we convert Eq. (2.3) and express the Majoranas as a superposition of conventional fermions.

$$\gamma_A = i(c_x^\dagger - c_x) \quad \gamma_B = c_x + c_x^\dagger \quad (2.4)$$

The equation demonstrates that the  $\gamma$ -operators are equal to their Hermitian conjugate and therefore  $\gamma_{A,x}$  and  $\gamma_{B,x}$  represent even their own antiparticles. To go on, we determine the underlying anticommutation rule, where we need the conventional fermionic rules  $\{c_x, c_{x'}\} = 0$  and  $\{c_x^\dagger, c_{x'}\} = \delta_{x,x'}$ :

$$\begin{aligned} \{\gamma_{\alpha,x}, \gamma_{\alpha',x'}\} &= u_\alpha u_{\alpha'}^* \{c_x^\dagger, c_{x'}\} + u_\alpha^* u_{\alpha'} \{c_x, c_{x'}^\dagger\} \\ &= (u_\alpha u_{\alpha'}^* + u_\alpha^* u_{\alpha'}) \delta_{x,x'} \\ &= 2\Re(u_\alpha u_{\alpha'}^*) \delta_{x,x'} \\ &= 2\delta_{\alpha,\alpha'} \delta_{x,x'}, \end{aligned} \quad (2.5)$$

where  $\alpha$  indicates the Majorana operators ( $\alpha = A, B$ ),  $\Re$  stands for the real part of the term in the brackets and the two constants are defined through  $u_A = i$  and  $u_B = 1$ . This means that the  $\gamma$ -operators fulfill the conditions that are characteristic for Majorana fermions and we are able to infer that the  $\gamma$ -operators represent Majorana fermions. Thus, we have the ability to write ordinary fermions as a superposition of Majorana fermions, and we know how to transform a fermionic operator into Majorana space.

## 2.2 Majorana fermions in Kitaev's toy model

In this section, we introduce Kitaev's toy model [1] and we study the model with respect to the existence of Majorana fermions. In particular, we will study the model at two characteristic points that allow the existence of Majorana fermions, even in this simple model. Considering the two points, it will turn out that the system can be realized in two different topological phases.

We start with the introduction of Kitaev's toy model by following the review paper by Alicea [4]. The model describes fermions in a 1D spinless  $p$ -wave superconductor, which only exist on a chain with  $N$ -sites. The fermions are able to hop between adjacent chain sites and long-range-ordered superconductivity is allowed. The resulting mean-field Hamiltonian can be written as

$$H = -\mu \sum_{x=1}^N c_x^\dagger c_x - \frac{1}{2} \sum_{x=1}^{N-1} (t c_x^\dagger c_{x+1} + \Delta e^{i\phi} c_x c_{x+1} + \text{H.c.}), \quad (2.6)$$

where  $c_x$  describes the annihilation and  $c_x^\dagger$  the creation of a spinless fermion at site  $x$ ,  $\mu$  describes the chemical potential,  $t \geq 0$  the adjacent hopping strength,  $\Delta \geq 0$  the  $p$ -wave pairing amplitude,  $\phi$  the induced superconduction phase and H.c. denotes the Hermitian conjugate. For simplicity, we have set the lattice constant to unity. In the following, we choose  $\phi = 0$ , since we will not change the associated physics by doing that.

The model Hamiltonian is given in the basis of conventional fermions. However, we are interested in studying the model with respect to the existence of Majorana fermions, for what we need to transform the Hamiltonian into the Majorana basis. Due to Eq. (2.3), we know how to express the fermionic operator in terms of Majorana operators. Inserting the relation in Kitaev's toy model, we obtain the Hamiltonian in the Majorana basis, where it reads

$$H = -\frac{\mu}{2} \sum_{x=1}^N (1 + i\gamma_{B,x}\gamma_{A,x}) - \frac{i}{4} \sum_{x=1}^{N-1} (\Delta + t)\gamma_{B,x}\gamma_{A,x+1} - \frac{i}{4} \sum_{x=1}^{N-1} (\Delta - t)\gamma_{A,x}\gamma_{B,x+1}. \quad (2.7)$$

Now, we are interested in the existence of Majorana fermions in the treated model. In particular, we are interested in the interaction between Majorana fermions. This interaction influences the space configuration of the Majoranas and the system can be realized in two different topological phases. We start the study with the first case, which belongs to the absence of the hopping term  $t$  and the  $p$ -wave pairing amplitude  $\Delta$  and a non-vanishing chemical potential  $\mu$ . Here, only the  $\mu$ -part of the Hamiltonian (2.7) remains

$$H = -\frac{\mu}{2} \sum_{x=1}^N (1 + i\gamma_{B,x}\gamma_{A,x}) = -\mu \sum_{x=1}^N c_x^\dagger c_x. \quad (2.8)$$

On the left-hand side, we see that the Hamiltonian only permits the interaction of Majorana fermions at the same lattice site  $x$ , which means that the two Majorana fermions at site  $x$  are coupled to each other (see Fig. 2.1). The coupling causes that the two Majoranas build a conventional fermion, which illustrates the right-hand side. The rewriting of the Hamiltonian follows Eq. (2.4). We also see that the spectrum shows a gap, since we need to pay an energy  $\mu$  to add a conventional fermion. The second situation is exemplified by  $\mu = 0$  and  $t = \Delta$ . Concerning this setting of the parameters, the Hamiltonian is given by

$$H = -\frac{it}{2} \sum_{x=1}^{N-1} \gamma_{B,x}\gamma_{A,x+1} = t \sum_{x=1}^{N-1} \left( \tilde{c}_x^\dagger \tilde{c}_x - \frac{1}{2} \right), \quad (2.9)$$

where we introduce new fermionic operators through  $\tilde{c}_x = \frac{1}{2}(\gamma_{A,x+1} + i\gamma_{B,x})$ . Here, the Hamiltonian only allows interactions between adjacent lattice sites and therefore Majorana fermions at adjacent sites are coupled to each other. But there are two Majoranas at the end of the chain (see Fig. 2.1) that are separated from the Hamiltonian. These two Majorana are unpaired and they appear as *zero-energy* modes, in contrast to the gapped spectrum of the conventional fermions.

Based on the appearance of unpaired or paired Majorana fermions, we have the ability to distinguish the system in two different topological phases. The topological phases are characterized through the existence of paired or unpaired Majorana fermions. We will pick up the topic of topological phases in Sec. 2.3, in a detailed way.

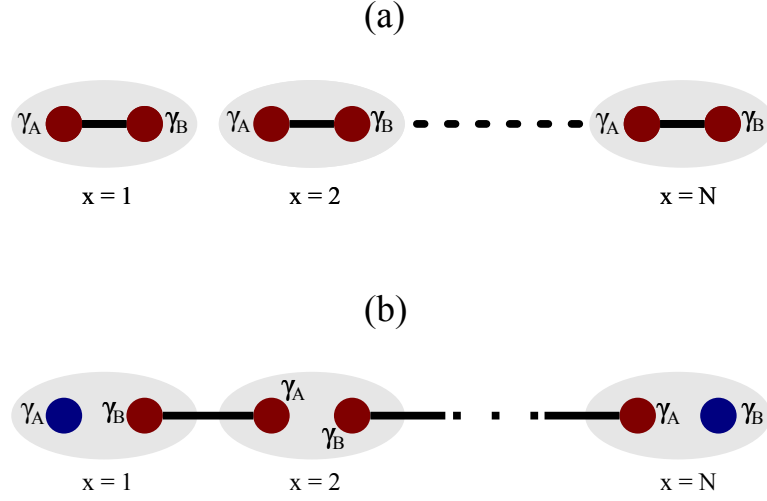


Figure 2.1: (a)  $\mu \neq 0$ ,  $\Delta = t = 0$ : Majorana fermions at the same lattice site are coupled to each other and there are no unpaired Majorana fermions in the system. (b)  $\mu = 0$ ,  $\Delta = t > 0$ : Majorana fermions at adjacent lattice sites are coupled to each other. This coupling results in the appearance of unpaired Majorana fermions at the end of the chain. The unpaired Majorana fermions are blue-colored.

## 2.3 Bogoliubov Transformation

In this section, we consider Kitaev's toy model with periodic boundary conditions and we determine the associated excitation spectrum, since we want to understand the model away from the two special points discussed above. We start the calculation of the spectrum with a transformation of Kitaev's model into its Bogoliubov-de Gennes form. The following Bogoliubov transformation gives us the possibility to determine the spectrum. Afterwards, we will use the properties of the excitation spectrum to explain the two topological phases.

To assume periodic boundary conditions, we need to add a term in Kitaev's model Hamiltonian. The resulting Hamiltonian reads

$$H = -\mu \sum_{x=1}^N c_x^\dagger c_x - \frac{1}{2} \sum_{x=1}^N (t c_x^\dagger c_{x+1} + \Delta c_x c_{x+1} + \text{H.c.}), \quad (2.10)$$



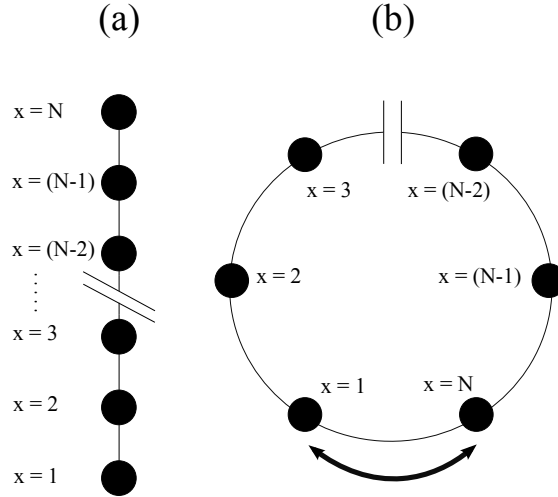


Figure 2.2: (a)  $N$ -site chain; (b) The figure demonstrates the periodic boundary conditions through transforming the chain into a loop. Now, interactions between the sites 1 and  $N$  are allowed.

where the parameters are already described. The addition causes that the second sum runs till lattice site  $N$  and allows interactions between site  $N$  and  $N+1$ . For simplicity, we achieve the assumption of periodic boundary conditions through the requirement that the creation and annihilation operators of site  $N+1$  are equal to the operators of site 1 ( $c_{N+1} = c_1$ ). The requirement can be understood by converting the chain into a ring (see Fig. 2.2). Because of the resultant translational invariance of the system, it is useful to switch into momentum space, which equals a discrete Fourier transform. The Fourier transform is given by  $c_x = \frac{1}{\sqrt{N}} \sum_{k \in \text{BZ}} e^{ikx} c_k$ , where  $c_k$  annihilates an electron of momentum  $k$ . Since the periodicity of the lattice causes that  $k$ -values that differ by a reciprocal lattice vector are identical, the summands are restricted to the first Brillouin zone according to  $k = \frac{2\pi}{N}j$  with  $-\frac{N}{2} < j \leq \frac{N}{2}$ , where we have assumed that  $N$  is an even number.

To express the Hamiltonian from Eq. (2.10), we substitute the operators through the

discrete Fourier transform. The technical procedure is shown for the hopping part in a detailed way below:

$$\begin{aligned}
 \sum_{x=1}^N c_x^\dagger c_{x+1} &= \sum_{x=1}^N \frac{1}{\sqrt{N}} \sum_{k \in \text{BZ}} e^{-ikx} c_k^\dagger \frac{1}{\sqrt{N}} \sum_{k' \in \text{BZ}} e^{ik'(x+1)} c_{k'}' \\
 &= \sum_{k \in \text{BZ}} \sum_{k' \in \text{BZ}} e^{ik'} c_k^\dagger c_{k'}' \frac{1}{N} \sum_{x=1}^N e^{i(k'-k)x}.
 \end{aligned} \tag{2.11}$$

We make use of the representation of the *Kronecker*- $\delta$ , characterized by  $\sum_{x=1}^N e^{i(k'-k)x} = N\delta_{k',-k}$ , to simplify the relation. Finally, we obtain

$$\begin{aligned}
 \sum_{x=1}^N c_x^\dagger c_{x+1} &= \sum_{k \in \text{BZ}} \sum_{k' \in \text{BZ}} \delta_{k',-k} e^{ik'} c_k^\dagger c_{k'}' \\
 &= \sum_{k \in \text{BZ}} e^{ik} c_k^\dagger c_k.
 \end{aligned} \tag{2.12}$$

The transformation of the other operators is equivalent and is not shown in details. We have to rewrite the momentum-space operators from Eq. (2.12) to obtain the Bogoliubov-de Gennes form of Kitaev's model. In the transcription of the operators, we use that the  $k$ -summands are symmetric concerning  $k = 0$ , with exception of  $k = \pi$ . This  $k$ -summand plays no role for  $c_k c_{-k}$ .<sup>1</sup> Based on this inversion symmetry ( $k$  and  $-k$  can be switched without changing the system), we are able to split Eq. (2.12) into two sums. This sums differ through the permutation of  $k$  and  $-k$ . Using the anticommutation rule for fermions  $\{c_k, c_{k'}\} = 0$ , we get for the superconduction part

$$\begin{aligned}
 \sum_{k \in \text{BZ}} e^{-ik} c_k c_{-k} &= \frac{1}{2} \sum_{k \in \text{BZ}} e^{-ik} c_k c_{-k} + \frac{1}{2} \sum_{k \in \text{BZ}} e^{ik} c_{-k} c_k \\
 &= \frac{1}{2} \sum_{k \in \text{BZ}} e^{-ik} c_k c_{-k} - \frac{1}{2} \sum_{k \in \text{BZ}} e^{ik} c_k c_{-k} \\
 &= -i \sum_{k \in \text{BZ}} \sin(k) c_k c_{-k}.
 \end{aligned} \tag{2.13}$$

---

<sup>1</sup>From the equivalence of  $k$ -values that differ by a reciprocal lattice vector, it follows that  $k = -\pi \equiv \pi$ . It follows that  $c_\pi c_{-\pi} = c_\pi c_\pi = 0$ , which means that the  $k = \pi$  mode plays no role.

Now, we have seen how to transform the Hamiltonian into momentum space. Inserting all the gotten relations, the momentum-spaced Hamiltonian reads

$$\begin{aligned}
 H_k &= - \sum_{k \in \text{BZ}} \left[ \mu + t \cos(k) \right] c_k^\dagger c_k + \frac{1}{2} \sum_{k \in \text{BZ}} \left[ i \Delta \sin(k) c_k c_{-k} + \text{H.c.} \right] \\
 &= \sum_{k \in \text{BZ}} \epsilon_k c_k^\dagger c_k - \frac{1}{2} \sum_{k \in \text{BZ}} \left[ \tilde{\Delta}_k c_k c_{-k} + \text{H.c.} \right],
 \end{aligned} \tag{2.14}$$

where  $\epsilon_k = -\mu - t \cos(k)$  characterizes the energy, with respect to the Fermi level and  $\tilde{\Delta}_k = -i \Delta \sin(k)$  describes the modified  $p$ -wave pairing amplitude.

Defining the two dimensional vector operator  $C_k^\dagger = (c_k^\dagger, c_{-k})$ —called Nambu operator—and using the anticommutation rules  $\{c_k, c_{k'}\} = 0$ ,  $\{c_k, c_{k'}^\dagger\} = \delta_{k,k'}$ , the Hamiltonian in Eq. (2.14) can be expressed in its standard Bogoliubov- de Gennes form and becomes

$$H_k = \frac{1}{2} \sum_{k \in \text{BZ}} C_k^\dagger \mathcal{H}_{\text{BdG}} C_k + \frac{1}{2} \sum_{k \in \text{BZ}} \epsilon_k, \quad \mathcal{H}_{\text{BdG}} = \begin{pmatrix} \epsilon_k & \tilde{\Delta}_k^* \\ \tilde{\Delta}_k & -\epsilon_k \end{pmatrix}, \tag{2.15}$$

where we have used that  $\epsilon_k = \epsilon_{-k}$ , since  $\epsilon_k$  is an even function of  $k$ . Because of the introduction of the Nambu operators, the degrees of freedom of the system are doubled. The reason is the particle-hole symmetry of the resultant Hamiltonian, which means that we treat electron and hole states to describe the system. In reference to Sec. 2.1, electron and holes states are equal to each other and consequently, we double the degrees of freedom.

The obtained particle-hole symmetry can be used to perform a Bogoliubov transformation. The idea of a Bogoliubov transformation is the introduction of new quasiparticle operators, where the quasiparticles represent the excitation out of the ground state. Thereby, the quasiparticle operators consist of a superposition of electron and hole states. The quasiparticle operators have the form [4],[5]

$$\begin{aligned}
 a_k &= u_k c_k + v_k c_{-k}^\dagger, \\
 a_{-k} &= v_k c_k^\dagger - u_k c_{-k},
 \end{aligned} \tag{2.16}$$

where  $a_k$  describes the annihilation of a quasiparticle with momentum  $k$ ,  $c_k$  describes the annihilation of an electron state and  $c_{-k}^\dagger$  symbolizes the creation of a hole state. The superposition of electron and hole states causes a further enlargement of the

degrees of freedom by a factor 2. But through the introduction of the quasiparticles, we have the ability to diagonalize the Hamiltonian, since we can choose the coefficients  $u_k$  and  $v_k$ , so that the off-diagonal terms of the Hamiltonian vanish. However, the choice of  $u_k$  and  $v_k$  is not arbitrary, since we need to keep in mind that the quasiparticles have to fulfill the fermionic anticommutation rules. To satisfy that the quasiparticle operators conserve  $\{a_k, a_{k'}^\dagger\} = \delta_{k,k'}$ , we conclude

$$\begin{aligned} \{a_k, a_{k'}^\dagger\} &= \{u_k c_k + v_k c_{-k}^\dagger, v_{k'}^* c_{-k'} + u_{k'}^* c_{k'}^\dagger\} \\ &= u_k u_{k'}^* \{c_k, c_{k'}^\dagger\} + v_k v_{k'}^* \{c_{-k}^\dagger, c_{-k'}\} \\ &\Rightarrow 1 = |u_k|^2 + |v_k|^2. \end{aligned} \quad (2.17)$$

To go on in the diagonalization of the Hamiltonian, it is useful to write Eq. (2.16) in Nambu notation and one easily sees that the Nambu operators  $A_k$  and  $C_k$  are related by unitary transformation. In the space of  $A_k$ -operators, the Hamiltonian from Eq. (2.17) can be written as

$$\begin{aligned} H_k - \frac{1}{2} \sum_{k \in BZ} \epsilon_k &= \frac{1}{2} \sum_{k \in BZ} A_k^\dagger \mathcal{T}^\dagger \mathcal{H}_{BdG} \mathcal{T} A_k \\ &= \frac{1}{2} \sum_{k \in BZ} A_k^\dagger \mathcal{H}'_{BdG} A_k, \end{aligned}$$

$$\mathcal{H}'_{BdG} = \mathcal{T}^\dagger \mathcal{H}_{BdG} \mathcal{T}, \quad \mathcal{T} = \begin{pmatrix} u_k^* & v_k \\ v_k^* & -u_k \end{pmatrix}. \quad (2.18)$$

The obtained Hamiltonian still is characterized through particle-hole symmetry. As mentioned, we are able to choose the coefficients  $u_k$  and  $v_k$ , so that the off-diagonal terms of the Hamiltonian vanish. Thereby, particle-hole symmetry guarantees that we have to treat only one off-diagonal element, since the elements  $h_{12}^{\text{BdG}}$  and  $h_{21}^{\text{BdG}}$  are complex conjugate to each other. The vanishing element  $h_{12}^{\text{BdG}}$  reads

$$\begin{aligned} &\Rightarrow \tilde{\Delta}_k v_k^2 + 2\epsilon_k u_k v_k - \tilde{\Delta}_k^* u_k^2 \stackrel{!}{=} 0 \\ \Leftrightarrow \tilde{\Delta}_k^2 \left(\frac{v_k}{u_k}\right)^2 + 2\epsilon_k \tilde{\Delta}_k \left(\frac{v_k}{u_k}\right) - |\tilde{\Delta}_k|^2 &= 0 \\ \Leftrightarrow \tilde{\Delta}_k \frac{v_k}{u_k} &= -\epsilon_k \pm \sqrt{\epsilon_k^2 + |\tilde{\Delta}_k|^2}. \end{aligned} \quad (2.19)$$

Looking at Eq. (2.19), we have a second condition for the coefficients  $u_k$  and  $v_k$ . It is helpful to define  $E_{\text{Bulk}} = \sqrt{\epsilon_k^2 + |\tilde{\Delta}_k|^2}$ , which turns out to be the excitation energy. As mentioned earlier, the quasiparticles describe the excitation out of the ground state  $|\psi_0\rangle$ , which is defined through no excited electrons and fulfills  $a_k |\psi_0\rangle = 0$ . The ground state represents the lowest energy level, from which follows that  $E_{\text{Bulk}} \geq 0$ . If  $E_{\text{Bulk}}$  had been lower than 0, there would be quasiparticles even in the ground state, since it would cause a reduction in the energy. Hence, we disregard the negative square root in Eq. (2.19).

Combining Eq. (2.13) and Eq. (2.15), it is possible to determine terms for the coefficients  $u_k$  and  $v_k$ . They are in particular given by

$$\begin{aligned} u_k &= \frac{\tilde{\Delta}_k}{|\tilde{\Delta}_k|} \frac{\sqrt{E_{\text{Bulk}} + \epsilon_k}}{\sqrt{2E_{\text{Bulk}}}}, \\ v_k &= \left( \frac{E_{\text{Bulk}} - \epsilon_k}{\tilde{\Delta}_k} \right) u_k. \end{aligned} \tag{2.20}$$

After inserting Eq. (2.20) into the Hamiltonian, Kitaev's toy model is diagonalized. The final Hamiltonian can be written as

$$H_k = \sum_{k \in \text{BZ}} E_{\text{Bulk}} a_k^\dagger a_k + \frac{1}{2} \sum_{k \in \text{BZ}} [\epsilon_k - E_{\text{Bulk}}], \tag{2.21}$$

where the symmetry of  $E_{\text{Bulk}}(k)$  in  $k$  is used to simplify the equation. As one can see, the second sum symbolizes the energy of the ground state  $\langle \psi_0 | H_k | \psi_0 \rangle$  (with respect to the Fermi level), since in the ground state no quasiparticles exist. Here, it can be seen that the presence of superconductivity (described by the parameter  $\tilde{\Delta}_k$ ) leads to an energetic state below the Fermi level, in which the Cooper pairs can condense. Without the presence of superconductivity or at  $k = 0, \pi$ , there is no reduction in the ground state energy and the ground state is given by the Fermi level.

The first sum characterizes the excitation energy of the electrons with the help of quasiparticles. The spectrum is gapped, expect under special conditions, which we explain in the following. The system remains gapless, when  $E_{\text{Bulk}}(k)$  is equal to zero ( $E_{\text{Bulk}}^2(k)$  is either zero in this case):

$$E_{\text{Bulk}}^2(k) = \epsilon_k^2 + |\tilde{\Delta}_k|^2 \stackrel{!}{=} 0 \tag{2.22}$$

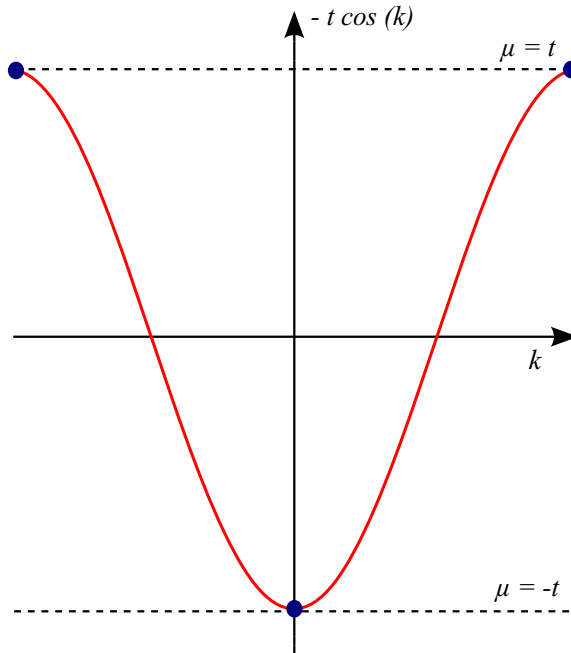


Figure 2.3: Plot of the kinetic energy in dependence of the momentum; only at the blue points a closure of the gap is possible. The blue points at  $k = \pi$  and  $k = -\pi$  are equivalent, since  $k$ -values that differ by a reciprocal lattice vector are equivalent. Between the dashed lines, the system is in the topological non-trivial phase, while outside the dashed lines the system is in the topological trivial phase.

Since  $E_{\text{Bulk}}^2(k)$  consists of two summands, both of them have to be equal to zero. First, we consider the superconduction part.  $|\tilde{\Delta}_k|^2$  is proportional to  $\sin^2(k)$  and thus, a closing of the gap is only possible at  $k = 0, \pi$ . It follows that the  $\epsilon_k$ -part has to vanish at the isolated points  $k = 0, \pi$ . Concerning  $k = 0$ ,  $\epsilon_k$  vanishes for a chemical potential that is tuned to  $\mu = -t$ . In contrast at  $k = \pi$ , the chemical potential has to be equal to  $\mu = t$ , so that  $\epsilon_k$  vanishes. Thus, we see that only at the Fermi level, a closure of the gap is possible.

In Sec. 2.1, we have seen that the creation and annihilation operators are related by  $\gamma(E) = \gamma^\dagger(-E)$  and that they only coincide at  $E = 0$ . With respect to Majorana fermions, it means that a closing of the gap is necessary for the appearance of unpaired Majoranas. This necessity of a closing gap causes that we cannot see unpaired Majorana fermions in the regime  $|\mu| > t$ . This coincides with our results from

Sec. 2.2 (first case:  $\mu \neq 0$  and  $t = 0$ ). Then, the system is realized in the topological trivial phase, characterized through the topological quantum number  $Q = 1$ , where  $Q = (-1)^m$  measures the parity of Majoranas at the end of the chain ( $m$  is the number of Majoranas at the end of the chain;  $m = 2$  in the topological trivial phase) [6],[7]. Concerning unpaired Majoranas, the reopening of the gap does not cause a vanishing of the *zero-energy* modes [3], when the gap is reopened with opposite sign with respect to the Fermi level. It means that unpaired Majorana fermions still exist in the regime  $|\mu| < t$ . This fact coincides with our treatment in Sec. 2.2 (second case:  $\mu = 0$  and  $t > 0$ ). In this case, the system is realized in the topological non-trivial phase, characterized through the topological quantum number  $Q = -1$  ( $m = 1$  because of unpaired Majoranas at the end of the chain). Thus, we can see a phase transition, when varying the chemical potential and passing  $|\mu| = t$ .

## 3 Majorana fermions with disorder

In this chapter, we will study Kitaev's model in presence of disorder. To simplify the analysis, we will analyze an effective low-energy model [8]. We will relate the topological quantum number  $Q$  to the reflection matrix of the system. Doing so, we will see that we need a transformation between transfer and scattering matrices, which we will determine. At least, the proper study of the disordered system will be done. In this section, we will determine a phase diagram that will visualize the appearance of unpaired Majorana fermions to the strength of disorder.

### 3.1 Low-energy Kitaev model

In this section, we will derive the low-energy version of Kitaev's toy model and we will explain, why we consider the low-energy version with respect to the appearance of Majorana fermions. In addition, we will determine the transfer matrix of the system, which we will need in the following sections to study the low-energy model in presence of disorder and in reference to existence of unpaired Majorana fermions.

After considering Kitaev's toy model in Sec. 2.2 with open boundary conditions and in Sec. 2.3 with periodic boundary conditions, we have seen that a closure of the excitation gap is necessary for the appearance of unpaired Majorana fermions. We have also seen that the closing of the gap is only possible at the Fermi level and we conclude that the interesting physics occurs around the Fermi level. Thus, we want to expand Kitaev's model around the Fermi momentum  $k_F$  (the Fermi momentum  $k_F$  represents the Fermi level). To expand Kitaev's model, we use the obtained Bogoliubov-de Gennes Hamiltonian from Eq. (2.15) and we execute a Taylor expansion of  $\epsilon_k$  and  $\Delta_k$  around the Fermi momentum  $k_F$  till the first non-vanishing order:

$$\begin{aligned}\epsilon_k &\approx \epsilon_{k_F} + t \sin(k_F)(k - k_F) = v_F p, \\ \Delta_k &\approx -i\Delta \sin(k_F) = -i \frac{v_F \Delta}{t} = -i\Delta_{k_F},\end{aligned}\tag{3.1}$$

where  $p = (k - k_F)$  characterizes the momentum with respect to the Fermi momentum,  $\Delta_{k_F} = \frac{v_F \Delta}{t}$  describes the modified superconduction parameter and  $v_F = t \sin(k_F)$  is



an abbreviation for the Fermi velocity. For simplicity, we do not differ between right-running and left-running modes, which means they correspond to the same Fermi velocity  $v_F$ . Furthermore, we have assumed that there is no mixing between electron and hole states, which is physically not correct. We will pick up the consequences of this assumption later. Inserting the relations into the Bogoliubov-de Gennes Hamiltonian, we obtain the low-energy version of Kitaev's toy model and it reads

$$\mathcal{H}_{BdG} \approx \begin{pmatrix} v_F p & -i\Delta_{k_F} \\ i\Delta_{k_F} & -v_F p \end{pmatrix} = v_F \tau_z p + \Delta_{k_F} \tau_y, \quad (3.2)$$

We note that the Hamiltonian still fulfills particle-hole symmetry, which is expressed by  $\mathcal{H}_{BdG} = -\mathcal{H}_{BdG}^*$ . In the last step, we have written the Hamiltonian in terms of the two Pauli matrices  $\tau_y$  and  $\tau_z$ . The Pauli matrices obey the relation  $\tau_i \tau_j = \delta_{ij} + i \sum_{k=1}^3 \epsilon_{ijk} \tau_k$ , which is useful in calculations with the Pauli matrices. Thereby,  $\epsilon_{ijk}$  stands for the Levi-Civita symbol, which is antisymmetric under every permutation of two indices. The Hamiltonian still exists on the lattice and the corresponding  $k$ -values (or rather the  $p$ -values from Eq. (3.1)) are still discrete (according to  $k = \frac{2\pi}{N}j$  with  $-\frac{N}{2} < j \leq \frac{N}{2}$ ). To be able to analyze the Hamiltonian analytically, we execute the continuum limit. The continuum limit is characterized through the limit, where  $N \rightarrow \infty$ . In this case, the  $p$ -values describe a continuous variable and we are able to solve the model analytically. After performing the continuum limit, the model describes an one-dimensional wire of length  $L$ , that still allows long-range-ordered superconductivity. We assume that the wire is located between  $x = 0$  and  $x = L$ .

To study the appearance of unpaired Majorana fermions, we are interested in the transfer matrix of the system. As mentioned in Sec. 2.1, particle-hole symmetry guarantees that Majorana fermions appear as *zero-energy* modes and therefore we are just interested in the transfer matrix at  $E = 0$ . We solve the eigenvalue problem in the position space—where we substitute  $p = -i\hbar\partial_x$  (since the momentum is continuous)—and it remains

$$\begin{aligned} \mathcal{H}\Psi(x) &\stackrel{!}{=} 0 \\ \Rightarrow \partial_x \Psi(x) &= -\frac{i}{\lambda_0} \tau_z \tau_y \Psi(x) \\ \Rightarrow \Psi(x) &= \underbrace{\exp\left[-\frac{x}{\lambda_0} \tau_x\right]}_{M(x)} \Psi(0), \end{aligned} \quad (3.3)$$

where the term under the brace stands for the transfer matrix and  $\lambda_0 = \frac{\hbar v_F}{\Delta}$  is the characteristic length of the system. In the last line, we have used the relation for the

$\tau$ -matrices given in the text above. One sees that the wave function is proportional to  $\Psi(0)$ , which directly implies the continuity condition at  $x = 0$ .

The exponential of the matrix is computed in a detailed way. Therefore, we make use of the series expansion of the exponential function and we separate the sum in an even and an odd part:

$$\begin{aligned}
 M(x) &= \sum_{n=0}^{\infty} \frac{\left(\frac{x}{\lambda_0} \tau_x\right)^{2n}}{(2n)!} - \sum_{n=0}^{\infty} \frac{\left(\frac{x}{\lambda_0} \tau_x\right)^{2n+1}}{(2n+1)!} \\
 &= \sum_{n=0}^{\infty} \frac{\left(\frac{x}{\lambda_0}\right)^{2n}}{(2n)!} \mathbb{I} - \sum_{n=0}^{\infty} \frac{\left(\frac{x}{\lambda_0}\right)^{2n+1}}{(2n+1)!} \tau_x \\
 &= \cosh\left(\frac{x}{\lambda_0}\right) \mathbb{I} - \sinh\left(\frac{x}{\lambda_0}\right) \tau_x.
 \end{aligned} \tag{3.4}$$

This is the transfer matrix at  $E = 0$ , which we need in the following process. We see that the matrix consists only of real elements and that the matrix is self-adjoint. These properties mean that we are in the Majorana basis, where all elements have to be real.

## 3.2 Scattering matrix

In this section, we will derive a relation between scattering matrix and transfer matrix. We will need the scattering matrix of the system, since we have the ability to link the determinant of the reflection matrix to the topological quantum number  $Q$  (see Sec. 3.3). Thus, the scattering matrix is able to indicate the existence of unpaired Majoranas. In addition, we will determine the scattering matrix of system that consists of more than one scatterer. This is important as the scattering matrix do not obey to a composition law.

In the last section, we have derived the transfer matrix of the low-energy version of Kitaev's model at  $E = 0$ . Here, we relate the elements of scattering matrix and transfer matrix to each other. Therefore, we consider the situation that is described in Fig. 3.1, where the scatterer is symbolized through the gray area [9]. There are four conductors, which represent the incoming and outgoing waves. The conductors have a fixed conducting direction. We are studying the transport on a mesoscopic level, which means that we are interested in evaluating the wave functions far away from the scatterer. In this region, only the superpositions of wave functions from two

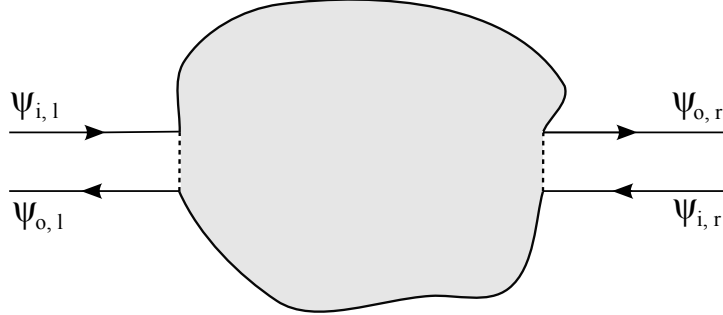


Figure 3.1: The gray area represents the scatterer. The four conductors represent the wave functions that pass the scatterer. Each of the conductors has a fixed conducting direction.

conductors are relevant. The scattering matrix describes the situation in a compact way and it is defined as

$$\begin{pmatrix} \psi_{o,l} \\ \psi_{o,r} \end{pmatrix} = \underbrace{\begin{pmatrix} r & t' \\ t & r' \end{pmatrix}}_{\mathcal{S}(E)} \begin{pmatrix} \psi_{i,l} \\ \psi_{i,r} \end{pmatrix}, \quad (3.5)$$

where we assume that every  $\psi$  stands for a  $n$ -dimensional vector that represent the  $n$  modes in the associated conductor, the subscripts  $i$  and  $o$  are abbreviations for incoming and outgoing waves and the subscripts  $l$  and  $r$  refer to the conductors on the left-hand side and right-hand side. Every matrix element constitutes a  $n \times n$  matrix. The element  $r$  describes the reflection from incoming waves on the left-hand side, while  $t$  describes the transmission from left-hand to right-hand side. The primed elements denote the scattering from the right-hand to left-hand side. The conservation of particle calls for the scattering matrix to be unitary ( $\mathcal{S}\mathcal{S}^\dagger = \mathcal{S}^\dagger\mathcal{S} = \mathbb{I}$ , where  $\mathbb{I}$  marks the identity). The unitary requires that the absolute value of the determinant is equal to 1 ( $|\det \mathcal{S}| = 1$ ).

In the definition of the scattering matrix, both sides are mixed. But there is another way to relate incoming and outgoing waves without mixing the sides. This way

uses the transfer matrix, which describes the transfer, e.g., from the left-hand to the right-hand side. Hence, the transfer matrix is defined as

$$\begin{pmatrix} \psi_{o,r} \\ \psi_{i,r} \end{pmatrix} = \underbrace{\begin{pmatrix} m_{11} & m_{12} \\ m_{21} & m_{22} \end{pmatrix}}_M \begin{pmatrix} \psi_{i,l} \\ \psi_{o,l} \end{pmatrix}, \quad (3.6)$$

The transfer matrix has the advantage of obeying a composition law, which means that the transfer matrix of a system, consisting of more than one scatterer, is multiplicative in contrast to the scattering matrix. Thus, we need a transformation from transfer to scattering matrices.

To construct such a transformation, we make use of the equations given by the definition of scattering and transfer matrix and we obtain

$$\psi_{o,r} = m_{11}\psi_{i,l} + m_{12}\psi_{o,l} \quad (3.7a)$$

$$\psi_{i,r} = m_{21}\psi_{i,l} + m_{22}\psi_{o,l} \quad (3.7b)$$

$$\psi_{o,l} = r\psi_{i,l} + t'\psi_{i,r} \quad (3.7c)$$

$$\psi_{o,r} = t\psi_{i,l} + r'\psi_{i,r}. \quad (3.7d)$$

The system of equations determines the demanded transformation. Thus, we combine Eq. (3.7b) and Eq. (3.7c), where we need to keep in mind the non-commutating property of multiplied matrices. The combination of the equations yields to

$$\begin{aligned} (1 - m_{22}t')\psi_{i,r} &= (m_{21} + m_{22}r)\psi_{i,l} \\ \Rightarrow m_{22} &= t'^{-1}, \quad m_{21} = -t'^{-1}r. \end{aligned} \quad (3.8)$$

In the last step, we require a vanishing of the multiplying factors, so that the above conditions can be satisfied for all  $\psi$ .

We need a relation for two further matrix elements and so we put Eq. (3.7a) on a level with Eq. (3.7d). In the obtained relation, we substitute  $\psi_{i,r}$  with the help of Eq. (3.7b). To simplify the condition, we utilize two properties that follow from the unitary of the scattering matrix (the exact derivation is arranged in the appendix) and the resultant elements are given by

$$\begin{aligned} (m_{12} - r'm_{22})\psi_{o,l} &= (r'm_{21} + t - m_{11})\psi_{i,l} \\ \Rightarrow m_{12} &= r't'^{-1}, \quad m_{11} = t^{\dagger-1}. \end{aligned} \quad (3.9)$$

However, physical processes are related to the scattering matrix, e.g., the electrical current through a system is naturally related to the transmission matrix of the system. And as mentioned earlier, we are able to link the reflection matrix to the topological quantum number. Thus, we need to invert the gotten relation and we obtain

$$r = -m_{22}^{-1}m_{21}, \quad t' = m_{22}^{-1}, \quad t = m_{11}^{\dagger-1}, \quad r' = m_{12}m_{22}^{-1}, \quad (3.10)$$

which describes the transformation from the transfer matrix to the corresponding scattering matrix. Now, we can determine the scattering matrix of the low-energy Kitaev model. Using the derived transformation, the scattering matrix of the treated system reads as  $E = 0$

$$\mathcal{S}(E = 0) = \begin{pmatrix} \tanh\left(\frac{L}{\lambda_0}\right) & \cosh^{-1}\left(\frac{L}{\lambda_0}\right) \\ \cosh^{-1}\left(\frac{L}{\lambda_0}\right) & -\tanh\left(\frac{L}{\lambda_0}\right) \end{pmatrix}, \quad (3.11)$$

where we have set  $x = L$  ( $L$  is length of the wire) and  $\lambda_0$  symbolizes the already defined characteristic length of the system. We easily check that the scattering matrix is unitary and that its determinant is equal to  $\det \mathcal{S} = -1$ , so that  $\mathcal{S}$  represents actually a scattering matrix. In particular, the scattering matrix of our system is a real matrix. The fact follows from being in the Majorana basis, which has to be real based on  $\gamma = \gamma^\dagger$  at  $E = 0$ .

The transformation will be insufficient, if the physical system consists of more than one scatterer, since the scattering matrix is not multiplicative ( $\mathcal{S} \neq \mathcal{S}_2\mathcal{S}_1$ ). To avoid the problem, we determine the transfer matrix of the total system and insert the gotten relations. The derivation can be found in the appendix. The resulting scattering matrix after two scattering processes can be written as

$$\mathcal{S}(E) = \begin{pmatrix} r_1 + t'_1(1 - r_2r'_1)^{-1}r_2t_1 & t'_1(1 - r_2r'_1)^{-1}t'_2 \\ t_2(1 - r'_1r_2)^{-1}t_1 & r'_2 + t_2r'_1(1 - r_2r'_1)^{-1}t'_2 \end{pmatrix}, \quad (3.12)$$

where the subscripted numbers denote the elements of the scattering matrices  $\mathcal{S}_1$  and  $\mathcal{S}_2$ . With respect to the low-energy Kitaev model, the total scattering matrix has the same look with the exception of substituting  $\lambda_0$  by the sum of reciprocal  $\lambda_{0,i}$  (in the derivation, we have used the addition theorems for hyperbolic functions).

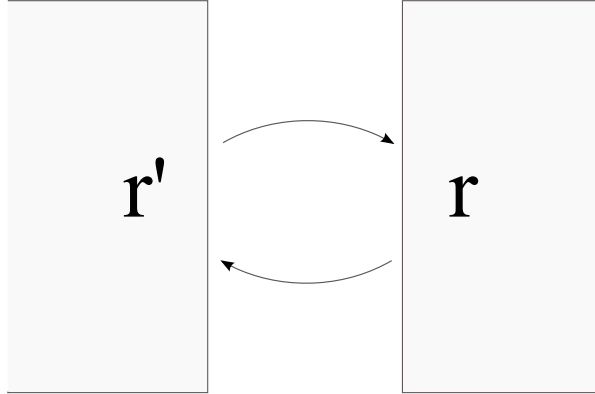


Figure 3.2: The gray areas symbolize the two wires and  $r, r'$  stands for the associated reflection matrices. To obtain an interface bound state, the state cannot change after two scattering processes at  $r$  and  $r'$ . The scattering processes are symbolized through the two arrows.

### 3.3 Relation between the reflection matrix and the topological quantum number

The section deals with a connection between the determinant of the reflection matrix and the topological quantum number  $Q$ . We will relate the two quantities to each other, so that we will be able to study the appearance of unpaired Majorana fermions with the help of the scattering matrix.

To get a relation between the determinant of the reflection matrix and the topological quantum number, we consider the situation that is shown in Fig. 3.2. With respect to Majorana fermions—which correspond to bound states at  $E = 0$ —we want to determine a condition for an interface bound state. An interface bound state in the system means that it cannot leave the area between the wires. Therefore, the corresponding wave function after two scattering processes has to fulfill  $rr'\psi = \psi$ , since the state does not change. The situation is similarly to an eigenvalue problem with eigenvalue  $\lambda = 1$  and there are non-trivial solutions for  $\det(\mathbb{I} - rr') = 0$ . This means that one eigenvalue  $\lambda$  of the matrix  $rr'$  has to be  $\lambda = 1$ . Since we calculate the scattering matrix in the Majorana basis, all matrix elements are real. It follows that the matrix  $rr'$  is an element of the orthogonal group  $O(2n)$ . Thereby, particle-hole symmetry guarantees that  $rr' \in O(2n)$ , since we consider particle and hole states. As the matrix  $rr'$  is an element of  $O(2n)$ , the determinant vanishes for

$$\det(rr') = \det(r) \det(r') = -1 \quad \Rightarrow \quad \det(\mathbb{I} - rr') = 0 \quad (3.13)$$

A detailed discussion about the relation can be found in the appendix. To obtain an interface bound state, Eq. (3.13) indicates that there is a restriction for the determinant of the reflection matrix, given by  $\det r = \pm 1$ . The property is similar to the topological quantum number  $Q = (-1)^m$  (where  $m$  is the number of Majoranas at the end of the wire), which either can be  $Q = \pm 1$ . As the restriction of the determinants is a condition for an interface bound state at  $E = 0$ , we conclude that the reflection determinant is equal to the topological quantum number and we identify  $\det r = Q_R$  (the index  $R$  indicates the topological quantum number of the right wire)[10]. In addition, Eq. (3.13) indicates that unpaired Majoranas only appear in one wire, e.g., in the right wire, since  $Q_R$  and  $Q_L$  ( $Q_L = \det r'$ ) are opposite in sign.

However, this argumentation is wrong in our case. Since we have assumed that there is no mixing between particle and holes states, the matrix  $rr'$  is not an element of the orthogonal group  $O(2n)$  any more. The disregard of particle-hole symmetry—which equals a bisection of the degrees of freedom—causes that  $rr'$  is an element of the orthogonal group  $O(n)$ . But we still need one eigenvalue with  $\lambda = 1$  to satisfy the determinantal condition. It follows that the determinantal condition reads in our case

$$\det(rr') = \det(r) \det(r') = +1 \quad \Rightarrow \quad \det(\mathbb{I} - rr') = 0 \quad (3.14)$$

The detailed discussion can also be found in the appendix. With respect to our model, we see that  $\det(r)$  and  $\det(r')$  have to be in sign. Since  $r$  and  $r'$  are opposite in sign, we see that a change in sign of the superconduction parameter  $\Delta$  is required (see Eq. (3.11)), so that the determinantal condition is fulfilled. We also identify  $\det r = Q_{L,R}$  for the left and the right wire. Since  $\det(r) = -\det(r')$ , the interface bound state condition reads  $Q_R Q_L = -1$  in terms of the topological quantum numbers. Here, we see that unpaired Majorana fermions only appear in one wire. This wire is characterized through a superconduction parameter  $\Delta < 0$  (since  $Q_R = \tanh\left(\frac{\Delta L}{\hbar v_F}\right) = -1$  in the topological non-trivial phase). The connection between topological quantum number and reflection matrix symbolizes the main point for our study of Majorana fermions with the help of scattering theory.

## 3.4 Disorder

In this short section, we define what we understand under the property of disorder, since we will study the low-energy in presence of disorder.

Disorder means that, e.g., the superconduction parameter  $\Delta$  is not a constant over the sample. In our case, the sample is equal to the wire. In theoretical physics, we need to average over all possible disorder configurations, so that a comparison between theory and experiment is possible, where a measurement over different disorder configuration is done. In the theory, we take the average over an ensemble of disordered system. In the end, the system can be either non self-averaging or self-averaging. The property of non self-averaging means that the presence of disorder is really important and the behavior of the system depends on the disorder configuration. In the case of non self-averaging quantities, the relative variance  $R_X = \frac{\sigma_{X,N}^2}{\langle X_N \rangle^2}$  of the quantity  $X$  tends not to 0 for large  $N$ , where  $N$  characterizes the number of ensembles. In contrast, a physical quantity can be self-averaging. In this case, the relative variance  $R_X$  tends to 0 for a large number  $N$  [11]. The system is then characterized through the expectation values of the several ensembles. In our study of disorder, we will assume that the expectation values and the deviations of the several samples are equivalent and we will see that the system will be self-averaging with respect to disorder in the superconduction parameter  $\Delta$ .

## 3.5 Result

In this section, we will treat the system with disorder. The disorder will be described in the superconduction parameter  $\Delta$  and we will study the appearance of unpaired Majorana fermions with respect to the strength of disorder. First, we will make a rough approximation to determine a reference value. Afterwards, we will prove our approximation with the help of numerical simulations. In the end, we will present a phase diagram that illustrates the existence of unpaired Majorana fermions in reference to the strength of disorder.

Here, we study the system with presence of disorder in  $\Delta$ <sup>1</sup> and we consider the system in the continuum limit. The continuum limit means that the system consists of a series connection of  $N$  wires with length  $L$ , where  $N$  describes a large number. Thereby, the wires differ in their configuration of disorder impurities. But we assume that the expected values  $\langle \Delta_i \rangle$  and the deviations  $\sigma_i$  ( $i = 1, \dots, N$  stands for the several wires)

---

<sup>1</sup>In the following, we assume that there is a clean wire in front of the disordered system. The clean wire is in the topological trivial phase with  $\Delta > 0$  and it deals as a reference for the disordered system.



do not vary about the several wires and we assume that there is no correlation between the different samples. Because of the connection between the determinant of reflection matrix and the topological quantum number, we want to calculate  $\det r$ . Based on the disorder, we have to calculate the expectation value of physical observables with respect to the probability density function. Since we consider a system of  $N$  wires with same expectation values  $\langle \Delta_i \rangle$  and same deviations  $\sigma_i$ , the central limit theorem predicts that the sum of these variables follows a Gaussian distribution with expectation value  $N\langle \Delta_i \rangle$  and variance  $N\sigma_i^2$  (the corresponding relative error is proportional to  $N^{-1/2}$ ). Thus, we need to calculate

$$\langle \det r \rangle = \lim_{N \rightarrow \infty} \frac{1}{\sqrt{2\pi}\sigma} \int_{\mathbb{R}} \tanh\left(\frac{\Delta L}{\hbar v_F}\right) \exp\left(-\frac{(\Delta - \bar{\Delta})^2}{2\sigma^2}\right) d\Delta, \quad (3.15)$$

where we have used the abbreviations  $\bar{\Delta} = N\langle \Delta_i \rangle$  and  $\sigma^2 = N\sigma_i^2$ . In the continuum limit, where  $N$  tends to  $\infty$ , the width of the Gaussian function decreases and only a small regime around the expectation value is of interest for the integration, as the relative error is proportional to  $N^{-1/2}$ . Thus, to make a first approximation, we approximate the Gaussian function through a  $\delta$ -distribution. For the reflection determinant, we obtain

$$\langle \det r \rangle \approx \lim_{N \rightarrow \infty} \tanh\left(N \frac{\langle \Delta_i \rangle L}{\hbar v_F}\right) \hat{=} \text{sign}(\langle \Delta_i \rangle) \quad (3.16)$$

To verify that the approximation is valid, numerical calculations have been done. Therefore, a short program is written, which can be executed in *root*. The program is explained below.

```
cout << "Please enter left and right bounds : ";
cin >> left >> right;
cout << "Please enter a number of partitions (> 0) : ";
cin >> R;
```

In the beginning, the bounds of integration and the number of partitions  $R$ , which describes the fineness of the integration, are imported.

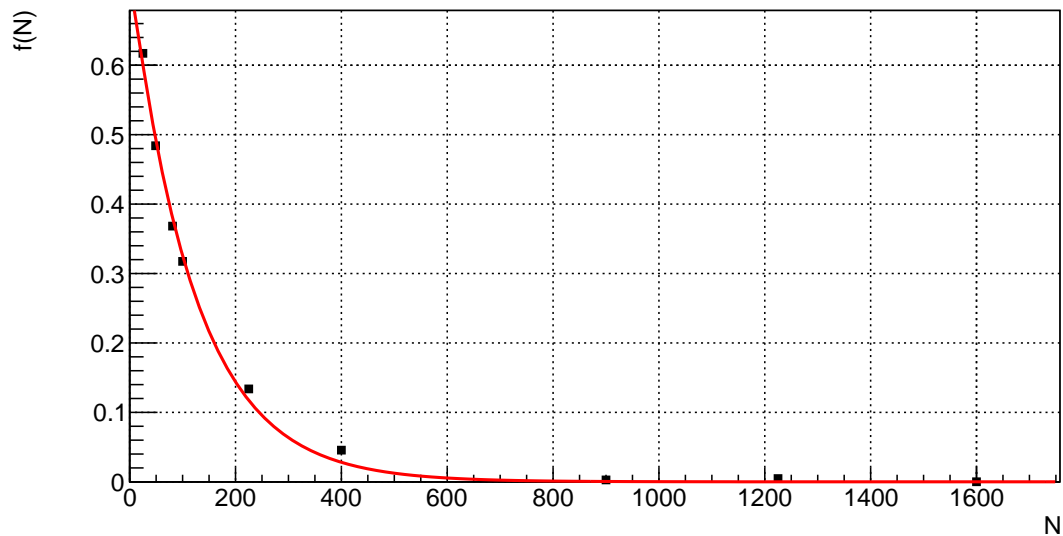


Figure 3.3: Result of the numerical simulation with the following parameters:  $\frac{\hbar v_F}{L} = \langle \Delta_i \rangle$ ,  $\sigma_i = 10 \langle \Delta_i \rangle$ ,  $\langle \Delta_i \rangle > 0$ . In the figure, the difference to +1 is shown and we have fit an exponential function at the data.

```
float width = (right - left)/R;
for(int i = 0; i < (R + 1); ++ i) [
total += func(left + width * i); ]
cout << "The integral is:" << total * width << endl;
```

The `for`-loop is the main part of the program. Here, the integral is calculated. Therefore, the function `func` is evaluated at `R` different points with the step size `width`, starting at the lower bound of integration. The single evaluations are stored in `total`, where they are added. In the last line, the value is displayed.

```
float func (float x) [
return tanh( $\sqrt{N}\sigma * x + N\mu$ ) * exp((-1) * (x * x)/2) *  $\sqrt{(2\pi)^{-1}}$ ; ]
```

In these lines, the integrand is defined and the computation is stored as return value.

Since we expect for the continuum limit that the reflection determinant is  $\pm 1$ , we can plot the difference to  $\pm 1$  for every  $N$  to get a qualitative impression. Fig. 3.3 and

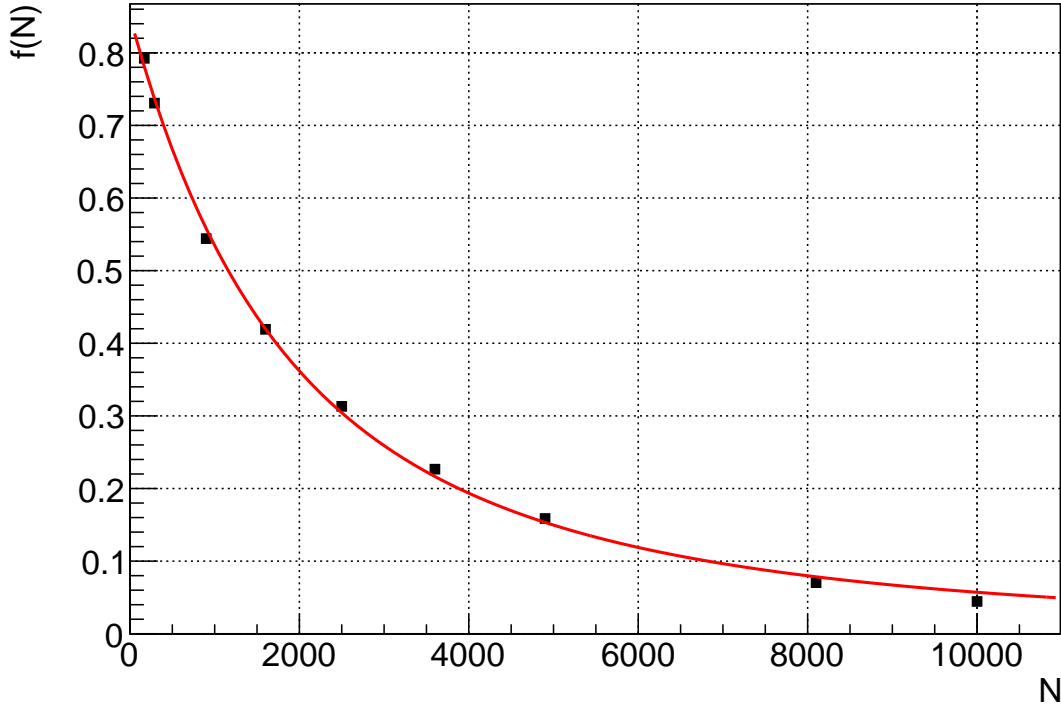


Figure 3.4: Result of the numerical simulation with the following parameters:  $\frac{\hbar v_F}{L} = |\langle \Delta_i \rangle|$ ,  $\sigma_i = 50 \langle \Delta_i \rangle$ ,  $\langle \Delta_i \rangle < 0$ . Here, the difference to  $-1$  is shown.

Fig. 3.4 show the plots that result from the numerical calculations for two different impurities. The qualitative development can be studied by fitting a function at the data. As we can see, the data shows an exponential decreasing trend. Thus, the approximation in Eq. (3.16) is justified in the continuum limit, where  $N \rightarrow \infty$ .

Since we are interested in the appearance of Majorana fermions, we are able to discuss the results. We have shown that the determinant of the reflection matrix only depends on the sign of  $\langle \Delta_i \rangle$ , which means that the existence of Majorana fermions is independent of the strength of disorder in the continuum limit. Because of the relation between reflection determinant and topological quantum number  $Q$ , we have the ability to attach the two different phases to the sign of  $\langle \Delta_i \rangle$ . Due to  $Q = -1$  in the topological non-trivial phase, a negative  $\langle \Delta_i \rangle$  leads to the appearance of unpaired Majorana fermions and the system is arranged in the topological non-trivial phase. In contrast a positive leads to  $Q = 1$  and the system is arranged in topological trivial phase. Thus, we conclude that the system fulfills a phase transition, when passing  $\langle \Delta_i \rangle = 0$ . The result is visualized in a phase diagram that is shown in Fig. 3.5.

The phase diagram shows the two different phases of the system. The abbreviations

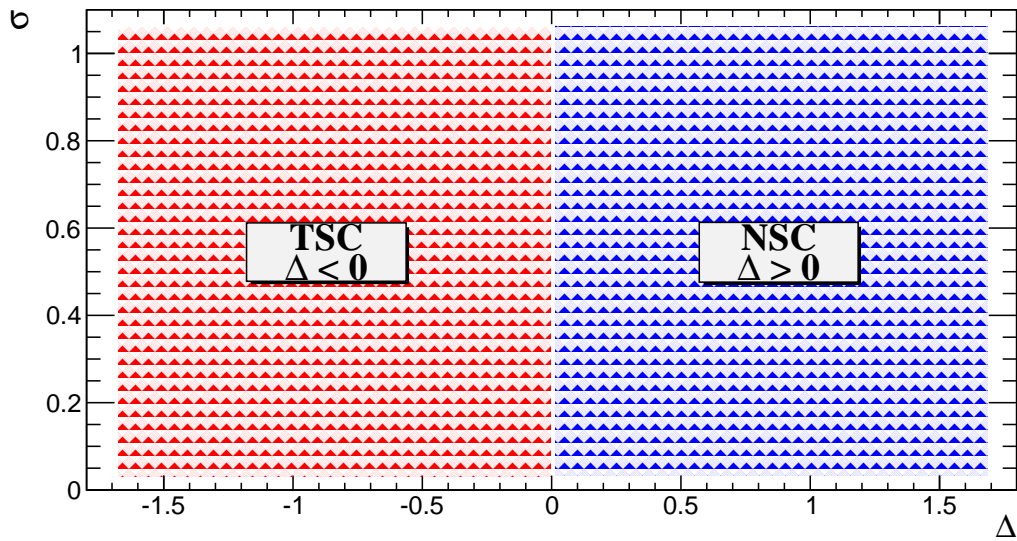


Figure 3.5: The Phase diagram of the disordered wire illustrates the appearance of unpaired Majorana fermions with respect to the strength of disorder  $\sigma$ ;  $\Delta < 0$  corresponds to the topological non-trivial phase, in which unpaired Majoranas exist;  $\Delta > 0$  corresponds to the topological trivial phase, in which only paired Majoranas exist. The abbreviation *TS* stands for topological superconductor, while *NS* stands for normal superconductor.

*NS* stands for normal superconductor and it describes that the system is in the topological trivial phase, where no unpaired Majoranas exist. The abbreviation *TS* stands for topological superconductor, since the system is in the topological non-trivial phase and there are unpaired Majorana fermions at the end of the wire.

## 4 Conclusion and Outlook

In the conclusion, we summarize the main results that we have obtained in the thesis. At the beginning, we have seen that we have introduced particles that are equal to their antiparticle, which are called Majorana fermions, and we have presented the operators through a sum of conventional fermionic operators.

Subsequently, we have studied the new operators in Kitaev's toy model with open and periodic boundary conditions and we have seen that Kitaev's model allows the appearance of unpaired Majorana fermions.

Furthermore, we have determined a transformation between transfer matrix and scattering matrix and we have determined the scattering matrix of a system that consists of more than one scatterer.

In addition, we have derived a connection between the topological quantum number, which measures the parity of Majorana fermions, and the reflection determinant of the scattering matrix. With the help of this connection, we have studied the low-energy Kitaev model in presence of disorder. Concerning the existence of unpaired Majorana fermions, we have seen that the appearance of *zero-energy* modes is independent of the strength of disorder, when treating the system in the continuum limit. At least, we have visualized the result in a phase diagram. To conclude, we have seen that even in this simple model, it is possible to observe *zero-energy* modes that represent Majorana fermions.

In the end, we want to give an outlook in reference to the studied topic. It would be possible to study Kitaev's model without performing a Taylor expansion around the Fermi momentum. In addition, it would be possible to consider the system with presence of disorder in other parameters, e.g., disorder in the hopping strength  $t$ . Furthermore it would be possible to study the presence of disorder in several parameters, e.g., disorder in the superconduction amplitude  $\Delta$  and in the hopping strength  $t$ .

# Bibliography

- [1] A. Y. Kitaev, *Phys.-Usp.* *44*, 131 (2001)
- [2] M. Franz, *Physics* *3*, 24 (2010)
- [3] C. W. J. Beenakker, arXiv:1112.1950. (2012)
- [4] J. Alicea, arXiv:1202.1293. (2012)
- [5] M. Tinkham, *Introduction to Superconductivity*, Dover Books on Physics
- [6] M. Z. Hasan and C. L. Kane, arXiv:1008.2026. (2010)
- [7] X.-L. Qi and S.-C. Zhang, arXiv:1008.2026. (2010)
- [8] C. W. J. Beenakker, F. Hassler, A. R. Akhmerov, J. P. Dahlhaus and M. Wimmer, arXiv:1009.5542. (2010)
- [9] P. W. Brouwer, *On the Random-Matrix Theory of Quantum Transport*, University of Leiden, Dissertation (1997)
- [10] J. T. Chalker and F. Merz, *Phys. Rev. B* *65*, 054425, (2002)
- [11] S. Wiseman and E. Domany, arXiv:cond-mat/9506101, (1995)

# A Appendix

## A.1 Scattering theory

The appendix includes derivations that are too large for the main part of the thesis. Here, it is shown that the matrix element  $m_{11}$  is equal to  $t^{\dagger-1}$ . Therefore, the unitary of the scattering matrix is used. The first relation follows from the main diagonal of  $\mathcal{S}\mathcal{S}^\dagger$ , which equals the identity:

$$\begin{aligned} 1 &= r'r'^\dagger + tt^\dagger \quad |t^{\dagger-1} \quad (\text{from the right}) \\ \Leftrightarrow t^{\dagger-1} &= t + r'r'^\dagger t^{\dagger-1}. \end{aligned} \quad (\text{A.1})$$

Using a vanishing element from the secondary diagonal, the obtained relation reads

$$\begin{aligned} 0 &= r't'^\dagger + tr^\dagger \\ r't'^\dagger &= -tr^\dagger \quad |t'^{\dagger-1} \quad (\text{from the right}) \\ r' &= -tr^\dagger t'^{\dagger-1} \quad |h.c. \\ r'^\dagger &= -t'^{-1}rt^\dagger \quad |t^{\dagger-1} \quad (\text{from the right}) \\ \Leftrightarrow r'^\dagger t'^{\dagger-1} &= -t'^{-1}r \end{aligned} \quad (\text{A.2})$$

Inserting Eq. (A.2) in Eq. (A.1), we obtain the result for  $m_{11}$  which is given in Eq. (3.9). In addition, the scattering matrix of two-scatterer system is derived. Therefore, we make use of the composition law of the transfer matrix  $M = M_2M_1$ . Thereby, every transfer matrix element corresponds to an element of a scattering matrix. The resulting transmission matrices are given by

$$\begin{aligned} t'^{-1} &= -t_2'^{-1}r_2r_1't_1'^{-1} + t_2'^{-1}t_1'^{-1} \\ &= t_2'^{-1}(1 - r_2r_1')t_1'^{-1} \\ \Leftrightarrow t' &= t_1'(1 - r_2r_1')^{-1}t_2', \end{aligned} \quad (\text{A.3})$$

and

$$\begin{aligned}
 r' &= (t_2^{\dagger-1} r_1' + r_2' t_2'^{-1}) t_1'^{-1} t' \\
 &\stackrel{(A.1), (A.2)}{=} \left( t_2 r_1' + r_2' t_2'^{-1} (1 - r_2 r_1') \right) t_1'^{-1} t' \\
 &\Leftrightarrow r' = r_2' + t_2 r_1' (1 - r_2 r_1')^{-1} t_2'.
 \end{aligned} \tag{A.4}$$

The computation of the reflection matrix leads to

$$\begin{aligned}
 r &= t' t_2'^{-1} (r_2 t_1^{\dagger-1} + t_1'^{-1} r_1) = \\
 &\stackrel{(A.1), (A.2)}{=} t' t_2'^{-1} \left( r_2 t_1 + (1 - r_2 r_1') t_1'^{-1} r_1 \right) \\
 &\Leftrightarrow r = r_1 + t_1' (1 - r_2 r_1')^{-1} r_2 t_1.
 \end{aligned} \tag{A.5}$$

Thus, the scattering matrix of complex system is determined.

## A.2 Determinantal condition for orthogonal matrices

In Sec. 3.3, we have used that the determinantal conditions are different for matrices that are elements of  $O(n)$  and  $O(2n)$ . In this part of the appendix, we will show the reason for this.

In general, for every orthogonal matrix  $A \in O(n)$  exists a basis, in which the matrix can be written as

$$A \doteq \begin{pmatrix} D(\theta_1) & & & & & \\ & \ddots & & & & \\ & & D(\theta_i) & & & \\ & & & +1 & & \\ & & & & \ddots & \\ & & & & & -1 \end{pmatrix} \tag{A.6}$$

where the missing elements are 0 and  $D(\theta)$  stands for a two dimensional rotation matrix





$$A \doteq \begin{pmatrix} D(\theta_1) & & & \\ & \ddots & & \\ & & D(\theta_l) & \\ & & & +1 \end{pmatrix} \quad (\text{A.9})$$

We have used these conditions in Sec. 3.3. At least, we summarize the result from this section in one equation. The equation reads

$$\det(\mathbb{I} - A) = 0 \quad \Leftrightarrow \quad A \in O(n) \begin{cases} \det A = -1 & \text{if } n \text{ even,} \\ \det A = 1 & \text{if } n \text{ odd.} \end{cases} \quad (\text{A.10})$$

# Erklärung

Ich versichere, dass ich die Arbeit selbstständig verfasst und keine anderen als die angegebenen Quellen und Hilfsmittel benutzt sowie Zitate kenntlich gemacht habe.

Aachen, den 20. September 2012

---

Unterschrift